

# Restoration of diffracted far field at the output of circular diffraction waveplate

D Hovhannisyan<sup>1</sup>, N Tabiryan<sup>2</sup>, H Margaryan<sup>1</sup>, V Abrahamyan<sup>1</sup>,  
N Hakobyan<sup>1</sup>

<sup>1</sup>Yerevan State University, Radiophysics department, Yerevan, Armenia,  
<sup>2</sup>Beam Engineering for Advanced Measurements Co., FL, USA

E-mail: [davidhl@ysu.am](mailto:davidhl@ysu.am), [nelson@beamco.com](mailto:nelson@beamco.com)

**Abstract.** The light propagation in an anisotropic periodic media, such as circular diffraction waveplate (CDW) by a finite-difference time-domain (FDTD) technique is studied. The FDTD numerical simulation and the subsequent Fourier transform of the diffracted electric near field was been used for study of ability of CDW to diffract a laser beam and simultaneously convert polarization state. The FDTD simulation results used to restore the diffracted electric far field at the CDW output. an abstract.

## 1. Introduction

Most of circular diffraction waveplate CDW exhibit unique diffraction characteristics, such as polarization-independence, low scattering, and high diffractive efficiencies. For CDW the polarization conversion mechanism is determined by the spatial periodic distribution of the birefringence. The theoretical consideration is necessary to characterize the diffraction properties of CDW. One of the simplest and common methods to describe polarized light transmission is the Jones matrix based analysis, which easily reveals the polarization states of beams diffracted from the CDW but unfortunately cannot describe details of the optical electric field in and/or near the CDW. For optical systems the near fields distributions is important due to small sizes of modern photonics structures. A more practical approach to analyzing the detailed electric field in and/or near optical devices is given by the FDTD algorithm. This method present a powerful approach to directly solving Maxwell's equations both in time and space and are also applied to the analysis of arbitrary, anisotropic, and periodic structures [1]. Another advantage of FDTD techniques is their capability to visualize real-time pictures of the electromagnetic wave. In our early paper we reported that the FDTD can be adopted for understanding of some peculiarities of recording of CDW by doubling method [2]. In this paper, the FDTD method is used to analyze light propagation in CDW, and to restore the far field distribution.

## 2. FDTD numerical model for the description of CW linearly-polarized radiation propagation through the anisotropic periodic media

In this section the numerical analysis of light propagation through the CDW is presented. Let us consider the case when an arbitrary polarized beam of a continuous-wave (CW) laser with  $(E_x, E_y, 0)$  components propagates along  $z$  axis and hits a CDW (the problem's geometry is presented at Figure 1).



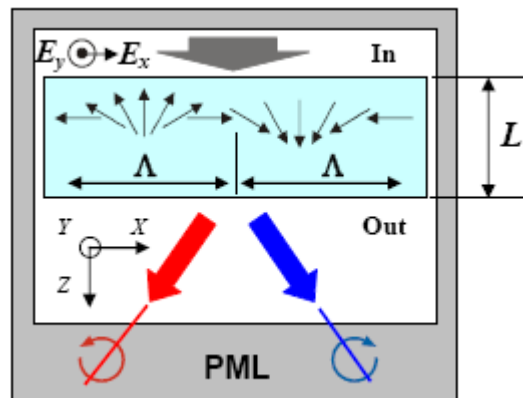


Figure 1 The schematic of CDW arrangement with respect to the coordinate axes.

The grating is placed in a position where the CDW molecules director's periodic change occurs in the  $x$  axis. Let's designate the grating's half-period as  $\Lambda$ , and the thickness as  $L$ . At the output of the grating the arrows show the propagation of radiation in  $-1$  and  $+1$  diffracted orders with left and right circular polarization. Generally Maxwell's equations for a periodic anisotropic medium can be written as follows:

$$\begin{aligned} \frac{\partial D_x}{\partial t} &= \frac{\partial H_z}{\partial y} - \frac{\partial H_y}{\partial z}, & \frac{\partial H_x}{\partial t} &= -\frac{1}{\mu} \left( \frac{\partial E_z}{\partial y} - \frac{\partial E_y}{\partial z} \right) \\ \frac{\partial D_y}{\partial t} &= \frac{\partial H_x}{\partial z} - \frac{\partial H_z}{\partial x}, & \frac{\partial H_y}{\partial t} &= -\frac{1}{\mu} \left( \frac{\partial E_x}{\partial z} - \frac{\partial E_z}{\partial x} \right) \\ \frac{\partial D_z}{\partial t} &= \frac{\partial H_y}{\partial x} - \frac{\partial H_x}{\partial y}, & \frac{\partial H_z}{\partial t} &= -\frac{1}{\mu} \left( \frac{\partial E_y}{\partial x} - \frac{\partial E_x}{\partial y} \right) \end{aligned} \quad (1) \quad (2)$$

where  $D_{x,y,z}$  are the electrical induction components,  $H_{x,y,z}$  are the magnetic field components,  $\mu$  is permeability of free space. The electric field vector can be described as  $E = \tilde{\epsilon}^{-1}D$ , where  $\tilde{\epsilon}$  is a permittivity tensor for a periodic anisotropic medium and which in the fixed laboratory system can be presented as

$$\epsilon(\varphi) = \begin{pmatrix} \epsilon_e \cos^2(\varphi) + \epsilon_o \sin^2(\varphi) & \Delta\epsilon \sin(\varphi)\cos(\varphi) & 0 \\ \Delta\epsilon \sin(\varphi)\cos(\varphi) & \epsilon_o \cos^2(\varphi) + \epsilon_e \sin^2(\varphi) & 0 \\ 0 & 0 & \epsilon_e \end{pmatrix} \quad (3)$$

where  $\epsilon_e, \epsilon_o$  are dielectric constants for extraordinary and ordinary waves,  $\Delta\epsilon = \epsilon_e - \epsilon_o$ , CDW molecule orientation related angles  $\varphi = \pi x/\Lambda, \alpha$ . According to (3), we consider the case when molecules lie in  $x$ - $y$  plane. The components of the electric field vector can be described as

$$\begin{aligned} E_x &= \tilde{\epsilon}_{xx}^{-1} D_x + \tilde{\epsilon}_{xy}^{-1} D_y + \tilde{\epsilon}_{xz}^{-1} D_z, \\ E_y &= \tilde{\epsilon}_{xy}^{-1} D_x + \tilde{\epsilon}_{yy}^{-1} D_y + \tilde{\epsilon}_{yz}^{-1} D_z, \\ E_z &= \tilde{\epsilon}_{xz}^{-1} D_x + \tilde{\epsilon}_{yz}^{-1} D_y + \tilde{\epsilon}_{zz}^{-1} D_z \end{aligned} \quad (4)$$

where the  $\tilde{\epsilon}_{xx}^{-1}, \tilde{\epsilon}_{xy}^{-1}, \tilde{\epsilon}_{xz}^{-1}, \tilde{\epsilon}_{yy}^{-1}, \tilde{\epsilon}_{yz}^{-1}, \tilde{\epsilon}_{zz}^{-1}$  are the components related to the permittivity inverse dielectric tensor. The essential feature in FDTD methods is a proper absorbing boundary condition (ABC) to truncate the simulation space without artificial reflections. Most often ABCs are used, which are based on the construction of artificial absorbing media in the truncated border domains. The

advantage of this idea is that the truncation can be made with orders of magnitude lower errors than employing one-way wave equations. The truncation border domains are filled virtually with a special anisotropic material for which it can be shown that a plane wave incident from vacuum with an arbitrary wave vector is transmitted without reflection. This phenomenon is referred to as perfect matching. In this article, we used the perfectly matched layer (PML, see Fig.1) introduced by Berenger [3]. Although at the gratings input we consider CW radiation with  $(E_x, E_y, 0)$  electric field components, due to the anisotropy of the grating (4), at the output of CDW the component  $E_z$  appear also. To calculate the diffracted field we make a transition from the continuous space  $(x, y, z, t)$  to the integer grid  $(i\Delta x, j\Delta y, k\Delta z, n\Delta t)$ , where  $i, j, k, n$  are integer constants [4]. The components of the electric and magnetic fields  $E$  and  $H$  will be interpolated at the time points  $n\Delta t$  and  $(n+1/2)\Delta t$  ( $n$  is a positive integer), respectively, where the constant time step  $\Delta t$  has to be chosen depending on the node distances and the refraction index. Discretization steps in the directions  $x, y$  and  $z$ , which are same  $\Delta x = \Delta y = \Delta z = \lambda_0/50$ ,  $\lambda_0 = 532$  nm is the CW radiation wavelength. With taking into account the inverse dielectric tensor

$$\begin{aligned}\tilde{\epsilon}_{xx}^{-1} &= [\epsilon_o \cos^2(\varphi) + \epsilon_e \sin^2(\varphi)] / \epsilon_o \epsilon_e, \\ \tilde{\epsilon}_{xy}^{-1} &= \tilde{\epsilon}_{yx}^{-1} = [-(\epsilon_e - \epsilon_o) \cos(\varphi) \sin(\varphi)] / \epsilon_o \epsilon_e \\ \tilde{\epsilon}_{yy}^{-1} &= [\epsilon_e \cos^2(\varphi) + \epsilon_o \sin^2(\varphi)] / \epsilon_o \epsilon_e, \tilde{\epsilon}_{zz}^{-1} = 1/\epsilon_e\end{aligned}\quad (5)$$

the electric field components calculated in accordance with (4).

### 3. Simulation results

In simulations considered the medium with  $n_e = 1.67$ ,  $n_o = 1.52$  and  $\Delta n = 0.15$  respectively. The grating's size in discrete numerical space along  $x$  axis was  $4\Lambda$ . In Figure 2 are shown the spatial distributions of the field components  $E_x(x, y)$ ,  $E_y(x, y)$  and their phase's  $angle(E_x(x, y))$ ,  $angle(E_y(x, y))$  inside and outside of CWD respectively for polarized input radiation

$E_x = \cos(\omega_0 t)$ ,  $E_y = \sin(\omega_0 t + \delta)$ ,  $\omega_0 = 2\pi c / \lambda_0$ ,  $\delta = 0; \pi/2; -\pi/2$ . The input and output boundaries of CWD are shown by white lines. The field components distributions along  $x$  axis immediately at the output of CWD, which preliminary are approximated by sin functions  $E_{x\_appr} = a_x \sin(b_x x + c_x)$ ,  $E_{y\_appr} = a_y \sin(b_y x + c_y)$  was used for restoration of diffracted far field.

The relative error of amplitudes  $(a_x - a_y) / a_x$  arising due to numerical calculations precision is no more than 1.73%, relative error of period along  $x$  axis  $(1/b_x - 1/b_y) / 1/b_x$  is no more than 1% and the relative error of phase difference  $(\pi - (c_x - c_y)) / \pi$  is no more than 0.3%. The direction along  $z$  axis is corresponding to the time scale. For generation the phase distribution of the field components the Hilbert transform was applied to each row ( $z$  axis) of field matrix. In that way was generated the new matrixes containing the complex values. The phase angles of these complex matrixes correspond to  $angle(E_x(x, y))$  and  $angle(E_y(x, y))$ , which containing information about the distribution of wave front delay along the  $x$  axis. According to simulation results and as seen from figure the  $angle(E_x(x, y))$  distribution along the  $x$  axis and at the fixed  $z$  value is shifted relative to  $angle(E_y(x, y))$  distribution by corresponding phase delay  $-0; \pi/2$  and  $-\pi/2$ .

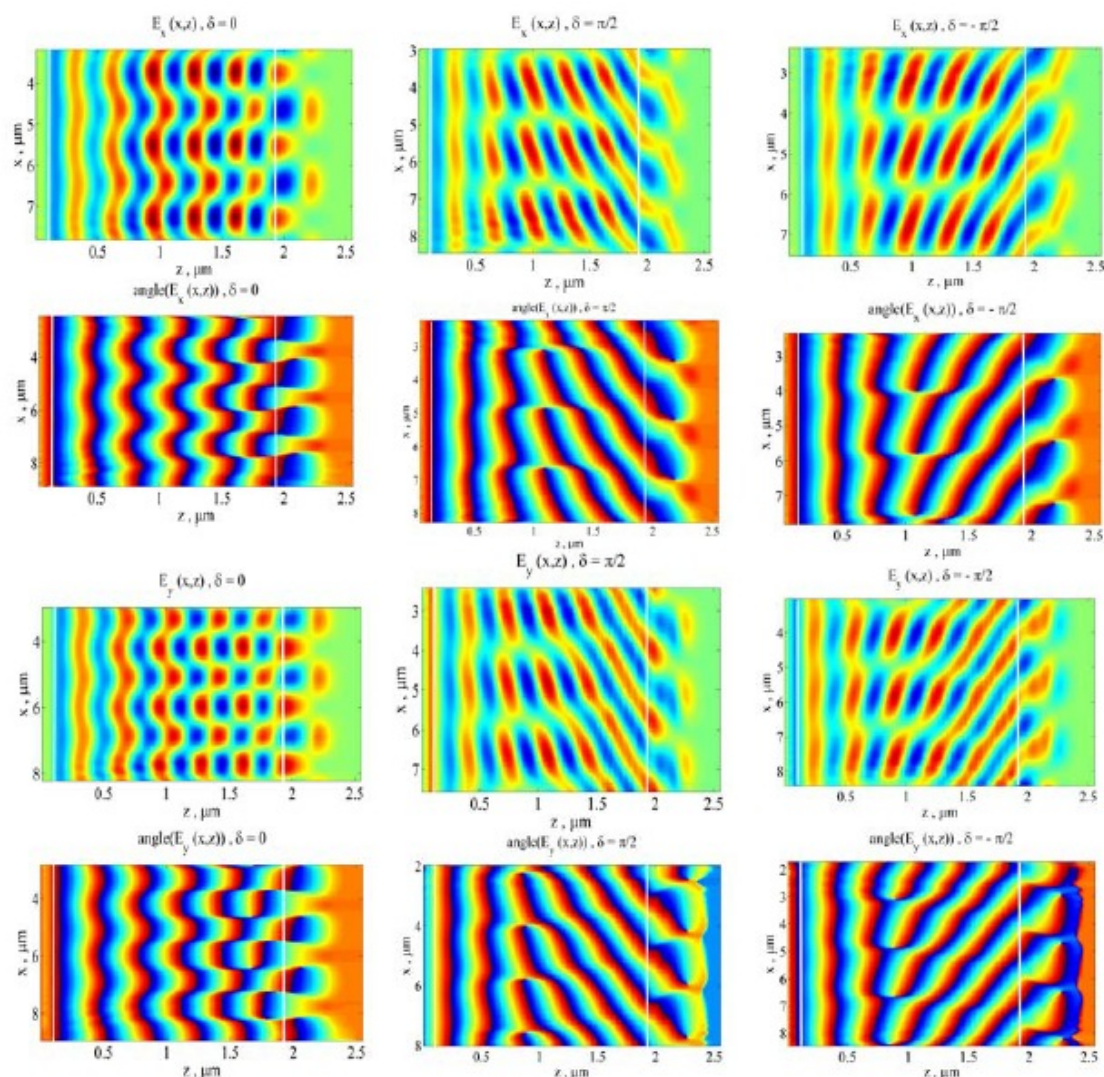


Figure 2 The field components and their phase's inside and outside of CDW for phase differences  $0; \pi/2$  and  $-\pi/2$  correspondingly.

### Conclusion

We have used the FDTD calculation of light propagation through the CDW by numerical solution of the Maxwell equations. For generation the phase distribution of the field components which containing information about the distribution of wave front delay along the  $x$  axis was applied the Hilbert transform. The restoration of diffracted far field at the output of CDW was done by Fraunhofer propagator.

This work is implemented in the frameworks of GIPP/ISTC A-1951 Project.

### References

- [1] Chulwoo Oh, Ravi Komanduri and Michael J. Escuti, , Physical Review A **76**, 2007, 043815.
- [2] Margaryan H. L., Aroutiounian V. M., Hovhannisyanyan D. L., Hakobyan N. H., Abrahamyan V. K., Mol. Cryst. Liq. Cryst., **559**, 2012, 214.
- [3] Jean-Pierre B'erenger, Perfectly Matched Layer (PML) for Computational Electromagnetics, Morgan & Claypool Publishers. 2007.
- [4] Allen Taflove and Susan C. Hagness, Computational Electrodynamics: The Finite-Difference Time-Domain Method, 3rd ed., Artech House Publishers, 2005.